Received: 2 November 2023 | Revised: 4 March 2024 | Accepted: 6 March 2024

DOI: 10.1002/esp.5830

RESEARCH ARTICLE

ESPL WILEY

Groundwater-surface water interaction, dissolved organic carbon oxidation and dissolution in carbonate aquifers

Andrew Oberhelman | Jonathan B. Martin | Madison K. Flint

Department of Geological Sciences, 241 Williamson Hall, PO Box 112120, University of Florida, Gainesville, FL, USA

Correspondence
Andrew Oberhelman, Department of Geological Sciences, 241 Williamson Hall, PO Box 112120, University of Florida, Gainesville, FL 32611-2120, USA.
Email: aoberhelman@ufl.edu

Funding information
Cave Research Foundation; University of Florida; National Science Foundation, Grant/Award Number: Grant EAR-1905259

Abstract

The high primary porosity and permeability of eogenetic karst aquifers permit water recharged through secondary dissolution features to be temporarily stored in aquifer matrix porosity. The recharged water contains elevated dissolved organic carbon (DOC) concentrations that, when oxidized, enhance limestone dissolution and impact carbon cycling. We evaluate the relationship between DOC oxidation and limestone dissolution using observations at a stream sink-rise system and reversing spring in the Floridan aquifer, north-central Florida, USA, where subsurface residence times of recharged water are days and months, respectively. We estimate water chemical compositions during surface water-groundwater interactions at these two systems with mixing models of surface water and groundwater compositions and compare them with measured DOC, dissolved inorganic carbon (DIC), Ca^{2+} and dissolved organic nitrogen (DON) concentrations. Differences between measured and modelled concentrations represent net changes that can be attributed to calcite dissolution and redox reactions, including DOC oxidation. DOC losses and Ca^{2+} gains exhibit significant ($p < 0.01$) inverse linear correlations at both the reversing spring (slope $= -0.9$, $r^2 = 0.99$) and the sink-rise system (slope $= -0.4$, $r^2 = 0.72$). DOC oxidation in both systems was associated with decreases in the molar C:N ratio (DOC:DON). Significant ($p < 0.01$) positive linear correlations between increases in Ca^{2+} and DIC concentrations after correcting for DIC derived from calcite dissolution occurred at both the reversing spring (slope $= 1.3$, $r^2 = 0.99$) and the sink-rise system (slope $= 1.61$, $r^2 = 0.75$). Greater deviations from the expected slope of -1 or $+1$ at the sink-rise system than at the reversing spring indicate DOC oxidation contributes less dissolution at the sink-rise system than at the reversing spring, likely from shorter storage in the subsurface. A portion of the deviation from expected slope values can be explained by the dissolution of Mg-rich carbonate or dolomite rather than pure calcite dissolution. Despite this, slope values reflect kinetic effects controlling incomplete consumption of carbonic acid during dissolution reactions.

KEYWORDS
carbonate dissolution, karst, organic carbon, oxidation, surface water-groundwater interactions

1 | INTRODUCTION

Oxidation of organic carbon (OC) is recognized as an important source of acidity driving dissolution in the subsurface of carbonate landscapes, particularly in eogenetic carbonates, which retain high primary porosity and permeability because of the lack of burial diagenesis (Choquette & Pray, 1970; Gulley et al., 2016, 2020; Vacher & Mylroie, 2002). In contrast, dissolution of telogenetic limestone, with low porosity and permeability because of recrystallization during burial, occurs as flow is focused along fractures, faults and bedding planes (Palmer, 1991). However, focused flow cannot concentrate dissolution in eogenetic limestone because the high porosity and permeability allow diffuse infiltration of water through the vadose zone, where acidity is lost as it dissolves limestone before it reaches

the water table (Gabrovšek & Dreybrodt, 2010). Thus, the model of focused dissolution developed in telogenetic karst requires revision to explain dissolution patterns in eogenetic limestone.

One proposed mechanism for concentrated dissolution in eogenetic limestones is mixing dissolution, where calcite undersaturation is generated by mixing two waters that have been equilibrated with calcite at different CO_2 partial pressures and/or ionic strengths. Mixing can generate calcite undersaturation because the solute concentrations (Ca^{2+} and CO_3^{2-}) of the mixture have linear relationships, while solute activity and calcite saturation are related by a power law (Bögli, 1964; Ford & Williams, 2007), thereby focusing dissolution in zones where mixing occurs. However, sufficient dissolution for speleogenesis in eogenetic carbonates requires idealized end member water compositions whereas measured solute concentration of end member water compositions fail to create enough calcite undersaturation to form observed cave sizes (Dreybrodt & Romanov, 2007; Gulley et al., 2016; Mylroie & Carew, 1990; Sanford & Konikow, 1989). A good example occurs in the Yucatan aquifer (Mexico) where mixing calculations of fresh and saline endmember water compositions were unable to cause undersaturation with respect to calcite (Gulley et al., 2016). Calcite undersaturation was found where simulated infiltrating water compositions were theoretically mixed with phreatic water sample concentrations from the water table of the Upper Floridan Aquifer (UFA, north-central Florida, USA). However, the undersaturation was insufficient to create dissolution rates that could form water table caves during periods of sea level stillstands when geomorphic evidence suggests the caves formed (Gulley et al., 2014).

Another cause of undersaturation and concentrated dissolution occurs at the water table, where heterogenous distributions of CO_2 develop along flow paths through variations in root respiration and the accumulation and microbial oxidation of OC (Cooper et al., 2016; Baldini et al., 2006; Gulley et al., 2020, 2016, 2015, 2014; Mattey et al., 2013; Whitaker & Smart, 2007; Wood, 1985). Dissolution occurs as water flows from regions of low to high CO_2 concentrations in the vadose zone, leading to CO_2 dissolution and hydration to carbonic acid (H_2CO_3). This mechanism results in 2–10 times more dissolution than the mixing of comparable source waters (Gulley et al., 2014; 2015). However, focused dissolution from OC oxidation likely depends on fractures, allowing CO_2 to migrate to the water table from regions of elevated respiration and CO_2 concentrations (Gulley et al., 2014; Mattey et al., 2013). This dissolution mechanism also requires sufficient terminal electron acceptor concentrations (e.g., O_2, NO_3^-, SO_4^{2-}, among others) to sustain microbial activity. Importantly, unlike in telogenetic karst, this model does not require focused inputs of calcite-undersaturated allogenic surface water for speleogenesis. Instead, speleogenesis occurs without hydrologic connections to surface drainages, which may form later due to erosion of the land surface (Gulley, Martin, Spellman, et al., 2013).

Once surface entrances form, caves often interact with surface runoff. One important interaction occurs as water levels of streams that receive spring discharge rise above the local water table and recharge surface water through the spring vent into the cave. These stochastic events of surface water-groundwater interaction (herein referred to as spring reversals) are recognized as an important driver of dissolution in eogenetic caves connected to the surface (Brown et al., 2014; Gulley et al., 2011; Moore et al., 2010; Screaton et al., 2004). Dissolution results from both the recharge of undersaturated surface water (Gulley et al., 2011) and in situ microbial oxidation of DOC supplied by the infiltrating water. However, the magnitudes of dissolution from OC oxidation have not been well quantified. Only a single study of one spring reversal has evaluated the contribution of DOC oxidation to dissolution through observations of corresponding changes in DOC, dissolved inorganic carbon (DIC) and Ca^{2+} concentrations (Brown et al., 2014). Although this result indicates DOC oxidation is important to dissolution, the relative magnitudes of DOC loss and limestone dissolution were not quantified.

The role of surface water-groundwater interactions in OC oxidation and calcite dissolution can be evaluated in the Suwannee River watershed (north-central Florida, USA) where eogenetic limestone of the Floridan aquifer is variably confined by semipermeable and impermeable siliciclastic rock. Where the aquifer is unconfined, numerous spring vents are proximal (<2-3 km) to the Suwannee River (Figure 1a, b). Allogenic runoff from the confined portion of the aquifer is undersaturated with respect to calcite and has elevated dissolved organic carbon (DOC) and terminal electron acceptor concentrations like dissolved oxygen and nitrate (Brown et al., 2014; Khadka et al., 2014; Moore et al., 2010). Spring reversals are common in the region because of this distribution of spring vents and the allogenic runoff generated on the confining unit (Brown et al., 2014; Gulley et al., 2011, 2013b) (Figure 2). Several stream sink-rise systems also exist at the boundary between confined and unconfined aquifers, with the largest on the Santa Fe River, a tributary to the Suwannee River (Figure 1d). At the Santa Fe River Sink-Rise system, flood events cause the hydraulic head in conduits to rise faster than the hydraulic head of the surrounding aquifer matrix and allow water to flow from the conduits into the aquifer matrix porosity (Bailly-Comte et al., 2010; Martin & Dean, 2001) (Figure 3). This water returns to the conduits during flood recession.

In this study, we investigate the role of the oxidation of DOC in dissolution using chemical mixing models and molar ratios of DOC, DIC, Ca^{2+} and dissolved organic nitrogen (DON) concentrations based on surface water-groundwater interactions in north-central Florida, USA. We hypothesize that the contributions of DOC oxidation to dissolution will form a linear relationship between the molar loss of DOC and the gain of solutes derived from limestone dissolution. The slope of this relationship should reflect the relative magnitudes of DOC oxidation and calcite dissolution, and the value of the slope should equal −1 if no other processes interfere. Further, microbial oxidation of DOC should impact the composition of residual dissolved organic matter (DOM) and would be reflected by a shift in the DOC:DON ratio. We also hypothesize that the relative magnitudes of redox and dissolution reactions should be controlled in part by the residence time of surface water in the subsurface and that shorter residence times would prevent reactions from reaching equilibrium depending on their reaction kinetics. We draw upon background data from 12 springs and a sink-rise stream system. We compare the Santa Fe River Sink-Rise system (herein, sink-rise system) and a spring reversal at Madison Blue Spring where subsurface water residence times for recharged surface water are days and months, respectively. This work addresses the relative importance of dissolution caused by OC oxidation in eogenetic karst and if this dissolution mechanism can focus on cave development and form high permeability flow paths in karst aquifers. Our results provide important context for the role of

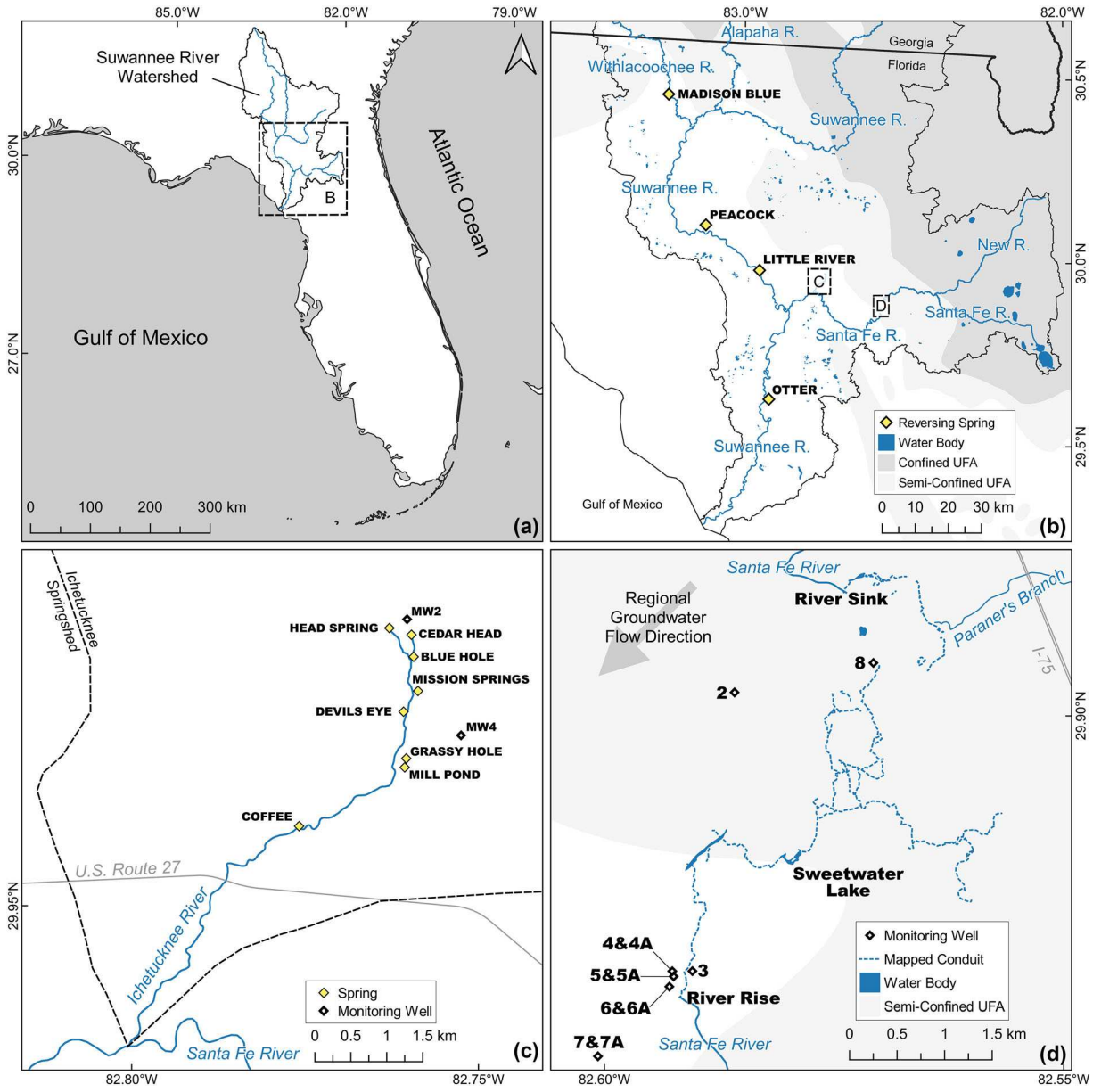

FIGURE 1 Map of the study area and sample sites. (**a**) Suwanee River watershed with the main study area outlined by the dashed box. (**b**) Map of the main study area in north central Florida showing the major drainages sampled reversing springs, and the Cody Scarp, which is approximately where the UFA is semi-confined. Locations of the Ichetucknee River (c) and the Santa Fe River sink-rise system (d) are outlined by dashed boxes. (**c**) Map of the Ichetucknee River and springshed showing sampled springs and two sampled monitoring wells. (**d**) Map of the Santa Fe River sink-rise system showing the three flow path sample points (river rise, Sweetwater Lake, river sink), mapped conduits (dashed lines) and sampled monitoring well locations (diamonds). Wells noted with an 'A' are screened at the water table. [Color figure can be viewed at wileyonlinelibrary.com]

surface water-groundwater interactions in karst aquifer carbon cycling (e.g., Martin, 2017).

2 | METHODS

2.1 | Study location

The study location is in the Suwannee River watershed in north-central Florida, USA (Figure 1). The entire watershed is underlain by the karstic Floridan aquifer, which consists of pre-Miocene eogenetic carbonate rocks that are confined in the northern portion by Miocene Hawthorn Group siliciclastic rocks and unconfined in the southern portion. A middle confining unit separates the Floridan aquifer into the UFA and the Lower Floridan aquifer. The UFA is composed of the Oligocene Suwannee and Eocene Ocala limestones and has porosities and matrix permeabilities around 30% and 10^{-13} m^2, respectively (Budd & Vacher, 2004). Ocala Limestone is >95% calcite by weight with trace amounts of clay, organics and dolomite (Schmidt et al., 1979). Suwannee Limestone is less pure with greater amounts of silica and is only present at one sampling location (Madison Blue Spring) (Schmidt et al., 1979; Williams & Kuniansky, 2015). The Hawthorn Group, which reaches a maximum thickness in north-central Florida of 95 m, has been completely removed by erosion in the southwestern region of the Suwannee River watershed thereby forming a geomorphic feature called the Cody Scarp that marks the boundary between confined and unconfined UFA (Figure 1b) (Scott, 1988). Where the Floridan

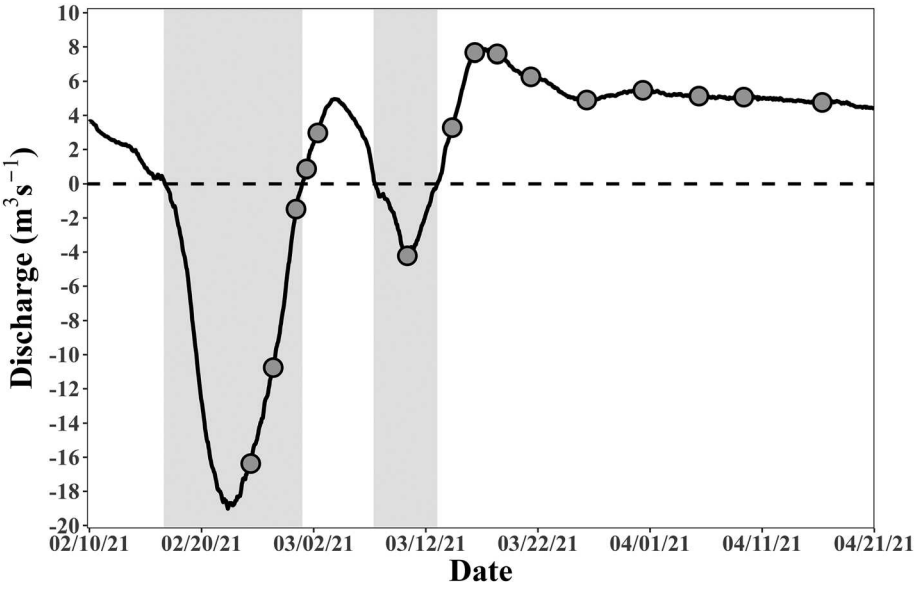

FIGURE 2 Hydrograph of the sampled 2021 spring reversal at Madison blue spring. Periods of negative discharge (grey-shaded regions) indicate when the Withlacoochee River stage exceeds the hydraulic head of groundwater at the spring vent allowing surface water to intrude into the spring system. The dashed line marks the shift between discharge and surface water intrusion at the spring vent. Samples collected during the reversal and recovery are marked as grey circles. Data are taken from USGS gauging station 02319302.

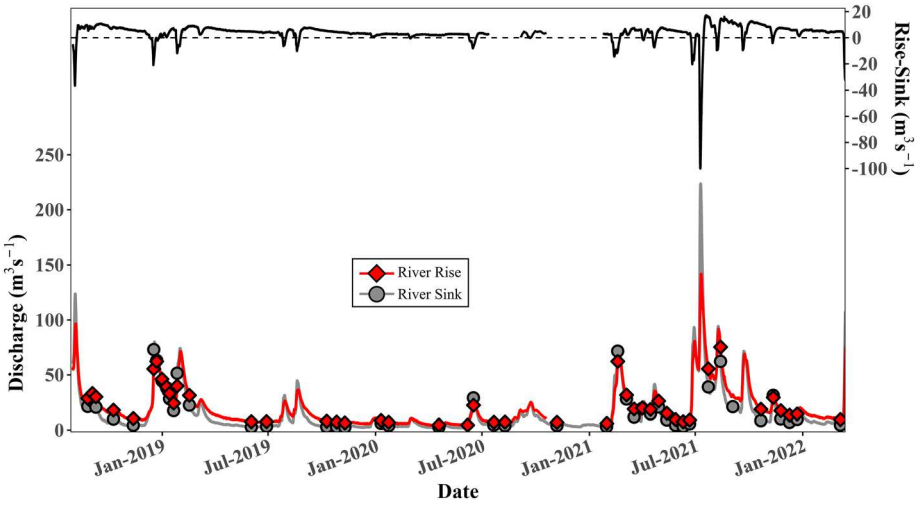

FIGURE 3 Hydrographs for the sink-rise system during the 2018–2022 study period. The grey line and grey circles represent river recharge into river sink (USGS gauging station 02321898) and times of sample collection, respectively. The red line and red diamonds represent river rise discharge (USGS gauging station 02321958) and times of sample collection, respectively. The black line in the upper panel represents the differences between river rise and river sink discharge with zero difference marked by the black dotted line. Negative values are interpreted to represent loss of water from the conduits to the matrix porosity and positive values are interpreted to represent gain of water from the matrix porosity to the conduits. [Color figure can be viewed at wileyonlinelibrary.com]

aquifer is confined, abundant surface water features form, including lakes and streams. Where the Floridan aquifer is unconfined, little surface water occurs and is limited to the Suwannee River, its major tributary, the Santa Fe River and small spring runs draining both rivers.

2.2 | Sampling locations

Samples were collected from Madison Blue Spring, Peacock Springs, Little River Spring, Otter Spring, eight vents in the Ichetucknee Springs group and the sink-rise system (Figure 1b–d). Groundwater samples were also collected from wells near Ichetucknee Springs and the sink-rise system and compared with legacy data from Floridan aquifer public supply wells that span all of Florida and into southern Georgia (McMahon et al., 2017). All sample locations have similar aquifer characteristics and semi-tropical climatic conditions because of their geographic proximity.

Otter Spring, Madison Blue Spring, Little River Spring and Peacock Spring are reversing springs classified as first (Madison Blue), second (Otter and Little River) or third (Peacock) magnitude, which have discharges of ≥2.8, 0.28–2.8 and 0.03–0.28 m^3/s, respectively (Meinzer, 1927). They discharge water to short spring runs (less than a few hundred metres) that flow to the Withlacoochee or Suwannee rivers (Figure 1b). Large floods on these rivers cause flow from the springs to reverse and recharge river water into the spring vent (Gulley et al., 2011). During baseflow periods these springs discharge water with subsurface residence times on the order of decades (Katz et al., 2001).

The Ichetucknee Springs group spring shed is in the unconfined portion of the Suwanee River watershed (Figure 1b,c) and receives little point recharge because of minimal surface drainage. As a result,

diffuse recharge is the dominant source for the discharging water and consequently, the mean apparent age of water discharging from the Ichetucknee Springs group ranges from 30 to 42 years (Martin et al., 2016). Sampled were collected from Head (second magnitude), Cedar Head (third magnitude), Blue Hole (first magnitude), Coffee (third magnitude), Mission (second magnitude), Devil's Eye (second magnitude), Grassy Hole (third magnitude) and Mill Pond (second magnitude) springs. Samples were also collected from two ~12 m deep and 10 cm diameter water table monitoring wells near Ichetucknee springs.

The Santa Fe River flows from the confined portion of the watershed onto the unconfined portion (Figure 1b,d). Where it crosses the Cody Scarp, a ~ 36 m deep sinkhole (River Sink) captures all of Santa Fe River flow, except during extreme floods when a small fraction of the river flows across the land surface. Water flows from River Sink through partially mapped anastomosing water-filled caves (herein called conduits) until it reemerges from a first magnitude spring (River Rise) ~ 8 km to the south that represents the headwaters of the lower Santa Fe River. The system of conduits connecting River Sink to River Rise has several collapse sinkholes that provide connections from the conduits to the surface, only one of which, Sweetwater Lake was sampled for this project. It occurs mid-way between River Sink and River Rise (Figure 1d). Gain or loss of water from the conduits is identified by the difference in river discharge measured at River Sink and River Rise, with losing conditions common during floods when flow captured by River Sink exceeds River Rise discharge (Bailly-Comte et al., 2010; Martin et al., 2006). Multiple groundwater monitoring wells are located near the mapped location of sink-rise system conduits. The wells are cased with 5.1 cm diameter PVC casing and extend either to the water table (~1–3 m below land surface) or to the depth of conduits (~30 m below land surface) (Ritorto et al., 2009).

During 2018–2020 and 2022, a total of 203 samples were collected at irregular intervals. During 2021, sampling occurred at regular intervals, with the sink-rise system sampled biweekly (Figure 3), the Ichetucknee Group springs sampled every four months and the reversing springs sampled every three months. Madison Blue spring reverses on average once or twice per year and one reversal was sampled between mid-February and mid-April, 2021, at an average rate of 1 sample every 4 days (Figure 2). Wells were sampled at least twice during 2020–2021. The accompanying data set contains exact sample dates and times.

2.3 | Field and laboratory methods

Water was pumped from spring vents, River Sink, Sweetwater Lake and River Rise using a Geotech peristaltic pump and weighted PVC tubing inserted into the water body. The pump outlet was connected to an overflow cup where a YSI ProQuatro Multiparameter Meter was used to monitor temperature, dissolved oxygen, specific conductivity and pH until values stabilized after which water samples were collected. Monitoring wells were sampled using a Proactive Environmental Products Submersible Tornado Pump with PVC tubing connected to an overflowing cup that contained the multiparameter metre electrodes. Samples were collected after purging at least three well-volumes and the multiparameter metre values stabilized.

All water samples collected for measurements of major ion (Ca^{2+}, Mg^{2+}, Na^{+}, K^{+}, Cl^{-}, SO_4^{2-}, F^{-} and NO_3^{-}), NH_4^{+}, DOC, total dissolved nitrogen (TDN) and DIC concentrations were filtered with in-line 0.45 µm GeoTech medium-capacity capsule filters. Major ion samples were collected in two 20 ml HDPE bottles. One sample bottle was acidified to pH < 2 in the field with trace-metal grade nitric acid and used for cation analyses and the other bottle was used for anion analyses with no added preservatives. Major ions were measured by ion chromatography on Dionex ICS-2100 (anions) and ICS-1100 (cations) instruments. NH_4^{+} samples were collected in 50 ml falcon tubes and frozen until measured by colorimetry on a Seal AA3 AutoAnalyzer (Method G-171-96). DOC and TDN samples were collected in 40 ml amber glass vials combusted at 550°C before use and were acidified with hydrochloric acid to pH < 2 in the field. DOC and TDN were measured on a Shimadzu TOC-VCSN total organic carbon analyser. Along with the in-line 0.45 µm GeoTech medium-capacity capsule filters, DIC samples were further filtered in the field with in-line 0.22 µM cellulose filters into 20 ml Qorpac glass vials and sealed with no headspace. DIC concentrations were measured on a UIC 5011 CO_2 coulometer coupled with an AutoMate Preparation Device. All samples were stored on ice in the field and refrigerated at 4°C or frozen (NH_4^{+} samples) upon return to the lab.

2.4 | DOC to DON ratios

DON concentrations were calculated as TDN minus the sum of NO_3^{-}-N and NH_4^{+}-N. The DOC:DON ratios were calculated in molar units for each sample and are hereafter referred to as C:N ratios. Of the 203 samples measured, 14 exhibited a negative DON concentration (TN < NO_3^{-}-N + NH_4^{+}-N) or C:N greater than 100 and were excluded from further analysis.

2.5 | Evaluation of OC cycling and dissolution

Chemical mixing models were used to separate chemical variations related to source water mixing from those resulting from biogeochemical and dissolution reactions during groundwater-surface water interactions at the sink-rise system and Madison Blue Spring. The sink-rise system model uses concentrations of SO_4^{2-} and Mg^{2+} to separate three sources of River Rise discharge, including (1) surface water recharging at the River Sink, (2) shallow groundwater represented by water collected at Well 4 and (3) deep upwelling mineralized groundwater represented by water collected at Well 2 (Moore et al., 2009). While redox and/or dissolution reactions may influence SO_4^{2-} and Mg^{2+} concentrations, both exhibit strong linear correlation between the three source waters indicating conservative behaviour at the sink-rise system (Moore et al., 2009). Additionally, unlike Cl^{-} and Na^{+}, which also behave conservatively, concentrations of SO_4^{2-} and Mg^{2+} have orders of magnitude differences between the three source waters, providing robust estimates of surface water and shallow groundwater contributions to the sink-rise system. Fractions of river water, shallow groundwater and deep groundwater were calculated by:

$$X_r = X_s + X_{w2} + X_{w4} \quad (1)$$

$$X_r Mg_r = X_s Mg_s + X_{w2} Mg_{w2} + X_{w4} Mg_{w4} \quad (2)$$

$$X_r SO_{4r} = X_s SO_{4s} + X_{w2} SO_{4w2} + X_{w4} SO_{4w4} \quad (3)$$

where the subscripts denote River Rise (r), River Sink (s), Well 4 (w4) and Well 2 (w2). X denotes the fraction of each endmember with X_r equal to 1. Mg and SO_4 denote the average concentrations of Mg^{2+} and SO_4^{2-} from samples at Well 4 and Well 2, while for River Sink and River Rise they denote the concentration of Mg^{2+} and SO_4^{2-} for the pairs of samples collected on the same day at River Sink and River Rise (Figure 3).

The Madison Blue Spring mixing model represents binary mixing between spring water and Withlacoochee River water. It is based on average Cl^- concentrations in groundwater discharging at the spring vent during baseflow (0.17 mM) and intruding river water (0.21 mM) during a spring reversal (Brown et al., 2014). Local diffuse recharge to the aquifer through the land surface is assumed insignificant relative to the volumes of groundwater and river water that mix during reversal. Fractions of river water and groundwater were calculated by:

$$1 = X_{gw} + X_{rw} \quad (4)$$

$$Cl_{obs} = X_{gw} Cl_{gw} + X_{rw} Cl_{rw} \quad (5)$$

where X_{rw} is the fraction of river water at the spring vent, X_{gw} is the fraction of baseflow groundwater at the spring vent, Cl_{obs} is the concentration of Cl^- measured in samples during the recession after reverse flow ends, Cl_{gw} is the average Cl^- concentration in spring discharge at baseflow and Cl_{rw} is the average Cl^- concentration of intruding river water.

Changes in the concentration of solutes related to biogeochemical or dissolution reactions (e.g., DIC, DOC, Ca^{2+}, etc.) were assessed by calculating Δ[x] values:

$$\Delta[x] = [x]_{observed} - [x]_{mix} \quad (6)$$

where [x] represents the concentration of the solute of interest and Δ[x] is the difference between the observed concentration ($[x]_{observed}$) and the concentration predicted by mixing of source waters ($[x]_{mix}$) based on Equations 1–5. Positive Δ[x] values represent a net gain of solutes from reactions and negative Δ[x] values represent a net loss of solutes from reactions. Δ[x] values of zero indicate conservative behaviour.

Molar relationships between the Δ[x] values for DIC, DOC and Ca^{2+} were used to assess OC cycling and its relationship to limestone dissolution or precipitation. First, we assume limestone dissolution or precipitation is represented by the dissolution or precipitation of calcite

$$CaCO_3 \leftrightarrow Ca^{2+} + CO_3^{2-} \quad (7)$$

which results in a ΔCa^{2+}:ΔDIC ratio equal to 1 and that the gain or loss of DIC by dissolution or precipitation is equal to the ΔCa^{2+} value (Equation 8):

$$\Delta DIC_{diss./precip.} = \Delta Ca^{2+}_{diss./precip.} \quad (8)$$

We estimate the gain or loss of DIC caused by DOC oxidation or autotrophy as the difference between the observed change in DIC (ΔDIC_{total}) and the change in DIC from dissolution or precipitation ($\Delta DIC_{diss/precip}$):

$$\Delta DIC_{oxid./auto.} = \Delta DIC_{total} - \Delta DIC_{diss./precip.} \quad (9)$$

Because potential losses of DOC through adsorption to Floridan aquifer material are small (0.67 mmol DOC kg^{-1} rock) (Jin & Zimmerman, 2010), we assume ΔDOC values relate only to oxidation or autotrophy:

$$\Delta DOC_{oxid./auto.} = \Delta DOC_{total} \quad (10)$$

Calcite can contain variable amounts of Mg^{2+} substituting for Ca^{2+} in the crystal lattice and limestones may also contain additional Mg^{2+} in the form of dolomite ($CaMg[CO_3]_2$). Dissolution of Mg^{2+} bearing carbonate minerals will influence molar relationships between Δ[x] values of DIC, DOC and Ca^{2+} (Equations 7–10). We thus include the effect of Mg^{2+} from limestone dissolution in our mass balance model as:

$$(Mg_x, Ca_{1-x})CO_3 \leftrightarrow xMg^{2+} + 1 - xCa^{2+} + CO_3^{2-} \quad (11)$$

where x is the mol% $MgCO_3$ in the limestone and from dolomite ($x = \sim 0.5$). Based on Equation 11, the ratio of DIC to the sum of Ca^{2+} and Mg^{2+} gained from dissolution is 1. Thus, subtraction and addition of ΔMg^{2+} values from $\Delta DIC_{oxid/auto}$ values and to $\Delta Ca^{2+}{}_{diss/precip}$ values, respectively, will refine Δ[x] value molar relationships to include the impact of Mg^{2+} related to limestone dissolution. This assessment is only made at Madison Blue Spring because the inclusion of Mg^{2+} in mixing models at the sink-rise system mixing model precludes the calculation of ΔMg^{2+} values.

We recognize that samples collected from River Sink and River Rise on the same day may not represent the same parcel of water and that, consequently, during periods of rapid changes in flow and associated rapid changes in chemical composition at River Sink lag those changes appearing at River Rise. An assessment of the impact of this lag on Δ[x] values of Ca^{2+}, DIC and DOC detailed in the Supporting Information indicates this sampling artefact has little impact on the results and we do not consider it further (Figures S1 and S2; Table S1).

2.6 | Subsurface residence time of water recharging the sink-rise system and Madison blue spring

Subsurface residence times at the sink-rise system were estimated from an established relationship between the time for temperature anomalies in water captured at River Sink to appear at River Rise and River Sink gage height (Bailly-Comte et al., 2011; Martin &

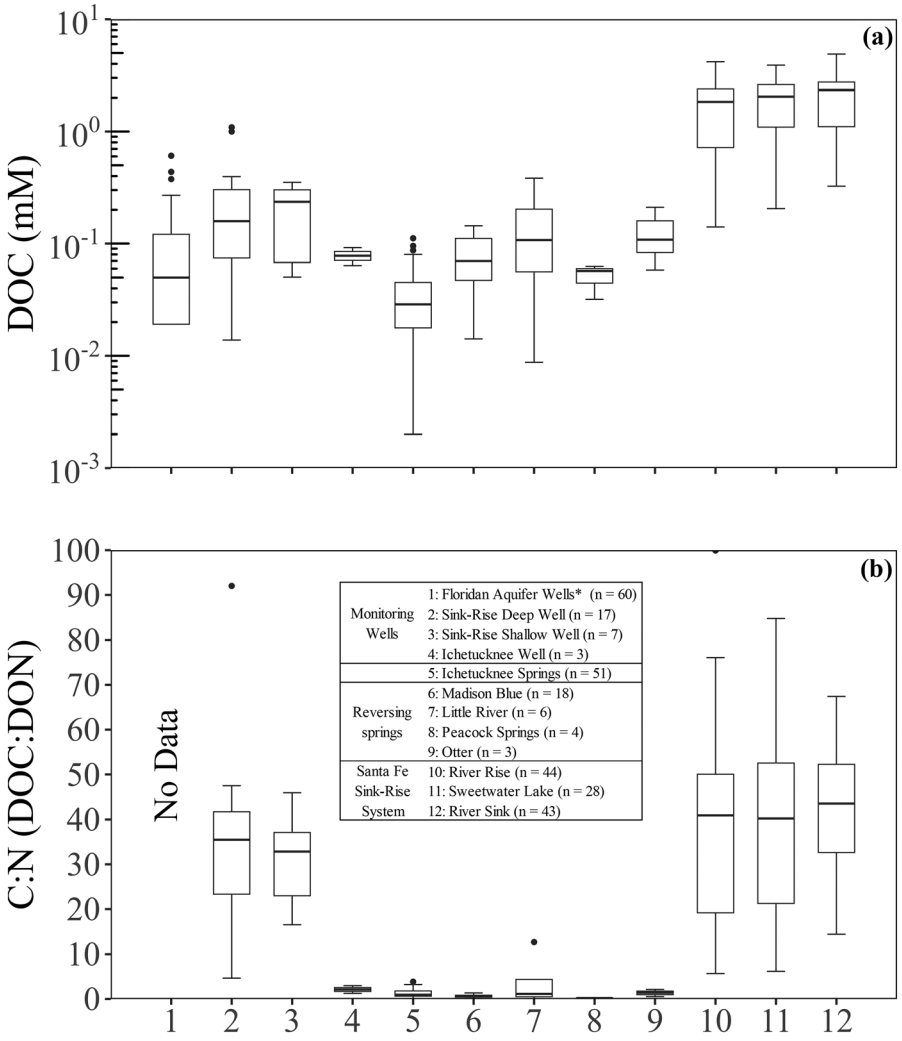

FIGURE 4 Boxplots of (**a**) DOC concentration on a log scale and (**b**) molar C:N by sampling location. Boxplots follow the standard Tukey definition. *Data from McMahon et al. (2017).

Dean, 1999, 2001). Residence times average 1.8 days and range between ~1 and 15 days, with an inverse exponential relationship with discharge. However, longer residence times are expected for water lost from the conduits to the matrix porosity (Martin & Dean, 2001).

The method for estimating the subsurface residence time of water recharged during the reversal at Madison Blue Spring is described in detail in the Supporting Information (Figure S3). Briefly, the estimates are based on a last in-first out accounting of the river water injected during reversal and river water returning to the surface after reversal, using the Cl^- mixing model (Equations 4–5) and the 15-minute discharge record from USGS gage 02319302 (Figure 2). Thus, the time that river water remains in the aquifer includes the amount of time between the end of the reversal and sample collection plus the time required to inject the same volume of river water during the reversal as had discharged following the end of the reversal. We refer to this time as the residence time.

3 | RESULTS

3.1 | DOC concentrations and C:N ratios

The DOC concentrations ranged from <0.01 to 4.89 mM for all samples, with the highest values where groundwater-surface water interactions are more frequent and recharged water has shorter subsurface residence times (Figure 4a). Ichetucknee group springs had the lowest median DOC concentration of 0.03 mM. The highest median DOC concentration of 2.41 mM occurred in river water at River Sink. Median DOC concentrations ranged from 0.06 to 0.11 mM at springs that experience reversals and from 0.05 to 0.24 mM in well waters, similar to reversing springs. The median DOC concentrations were higher in groundwater collected from both shallow (0.24 mM) and deep (0.16 mM) wells at the sink-rise system than median concentrations in reversing springs, waters collected from Ichetucknee wells (0.08 mM), and published concentrations from other Floridan aquifer wells (0.05 mM) (McMahon et al., 2017).

The C:N ratios of samples ranged from 0.2 to 99 (Figure 4b) and were lowest at Peacock springs (0.2) and highest at the sink-rise system. Median sink-rise system C:N ratios were 44 at River Sink, 40 at Sweetwater Lake and 41 at River Rise. Shallow and deep sink-rise system wells had median C:N ratios of 33 and 35, respectively. Median C:N values were less than 3.0 for reversing springs, Ichetucknee group springs and waters collected from Ichetucknee wells.

3.2 | ΔDOC values at the sink-rise system and Madison blue spring

Except for one sample time, the concentration of DOC at River Rise is less than the corresponding River Sink sample (e.g., Rise-Sink DOC < 0; Figure 5a). However, the ΔDOC values at River Rise show periods of

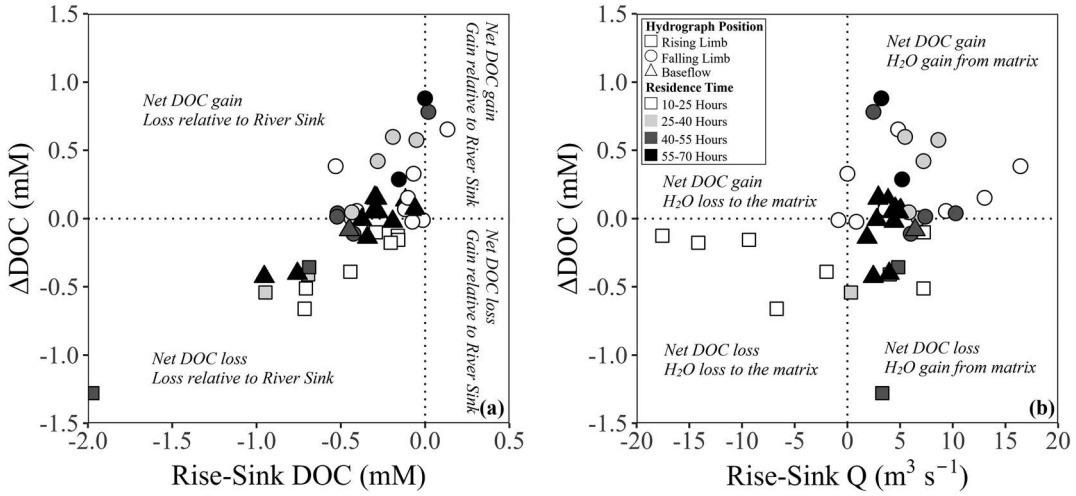

FIGURE 5 (**a**) ΔDOC values versus the difference in DOC concentration between River Sink and River Rise and (**b**) ΔDOC values versus the change in discharge between River Rise and River Sink. Data point shapes are determined by hydrograph position (e.g., Figure 3) and shaded according to residence time. Dotted lines mark Δ[x] values of zero.

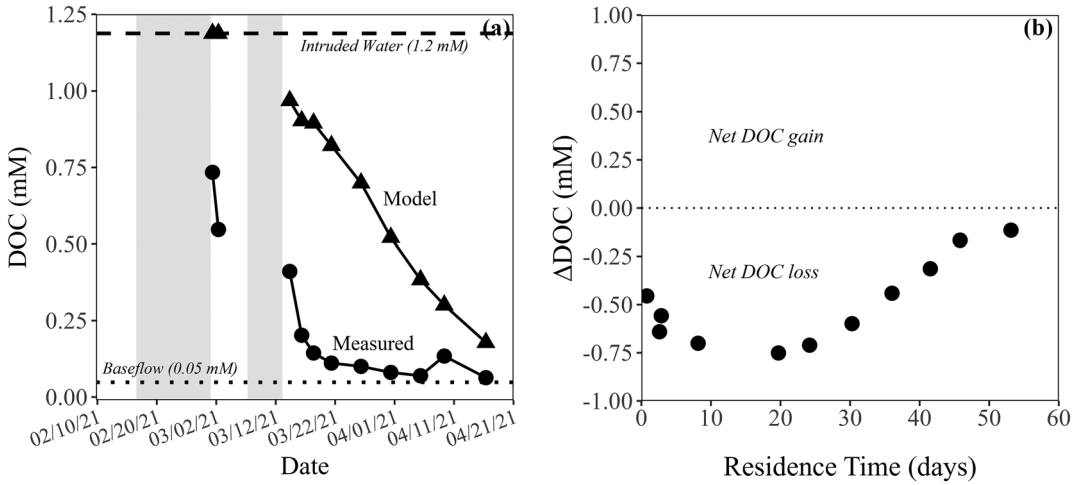

FIGURE 6 Time series and biplot for Madison blue spring after reversal. (**a**) Time series of measured (dots) and modelled (triangles) DOC concentration. Dashed and dotted lines mark mixing endmember compositions while the grey-shaded regions represent the periods of reversal. (**b**) Biplot of ΔDOC values versus injected water residence time (supplemental material). The dotted line marks a ΔDOC value of zero.

both net loss and net gain of DOC during flow through the sink-rise system. Net DOC loss (negative ΔDOC values) predominantly occurs on the rising limb of storm events while periods of net DOC gain (positive ΔDOC values) occur predominantly on the falling limb of storm events (Figures 3 and 5). During baseflow at the sink-rise system, when water residence times are longest, ΔDOC values tend to be close to zero representing no net change in DOC. The ΔDOC values show little systematic relationship with subsurface residence time. While DOC loss tends to occur on hydrograph rising limbs, as the magnitude of water loss from the conduit system to the aquifer matrix (Rise-Sink Q < 0; Figure 5b) increases, negative ΔDOC values trend towards zero. During periods when the conduit system gains water from the aquifer matrix (Rise-Sink Q > 0), ΔDOC values reflect both a net gain and a net loss of DOC regardless of hydrograph position.

The average DOC concentration of 1.2 mM in intruding surface water during the reversal at Madison Blue Spring is two orders of magnitude higher than the average DOC concentration of 0.05 mM of baseflow spring discharge (Figure 6a). Water discharging from the spring vent exhibits a rapid decline in DOC concentration after both periods of intrusion when flow resumed from the spring vent (Figure 2). A net loss of DOC (ΔDOC < 0) was observed in all samples collected after the spring reversal (Figure 6b). After the final period of intrusion, DOC concentrations return to near baseflow concentration ~8 days following the end of the reversal corresponding to a subsurface residence time of ~10 days. The maximum net loss of DOC occurred after ~20-day subsurface residence time when water discharging from the spring vent was ~70% injected surface water (Figure 6b). Following this maximum loss, increasing ΔDOC values indicate a return to baseflow groundwater discharge.

3.3 | $\Delta Ca^{2+}_{diss/precip}$, $\Delta DOC_{auto/oxid}$ and $\Delta DIC_{auto/oxid}$ relationships at the sink-rise system and Madison blue spring

Significant ($p < 0.01$) linear relationships exist between $\Delta Ca^{2+}_{diss/precip}$ (Equation 8) and $\Delta DOC_{auto/oxid}$ (Equation 10) and $\Delta DIC_{auto/oxid}$ (Equation 9) values at the sink-rise system (Figure 7) and Madison

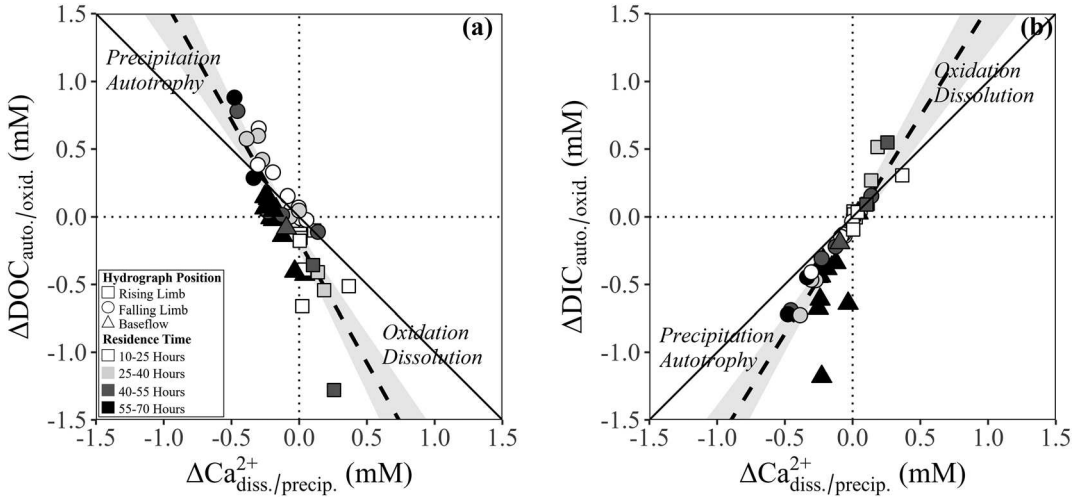

FIGURE 7 Data from the sink-rise system. (**a**) ΔDOC values related to oxidation and autotrophy (equation 9) versus ΔCa^{2+} values related to calcite dissolution and precipitation (equation 7) and (**b**) ΔDIC values related to oxidation and autotrophy (equation 8) versus ΔCa^{2+} values related to calcite dissolution and precipitation at. Data point shapes are determined by hydrograph position and shaded according to residence time. Dotted lines mark Δ[x] values of zero while the solid lines on (a) and (b) mark slopes of −1 and 1, respectively. Dashed lines represent linear regressions (Table 1) and the shaded grey regions represent the 0.95 confidence interval.

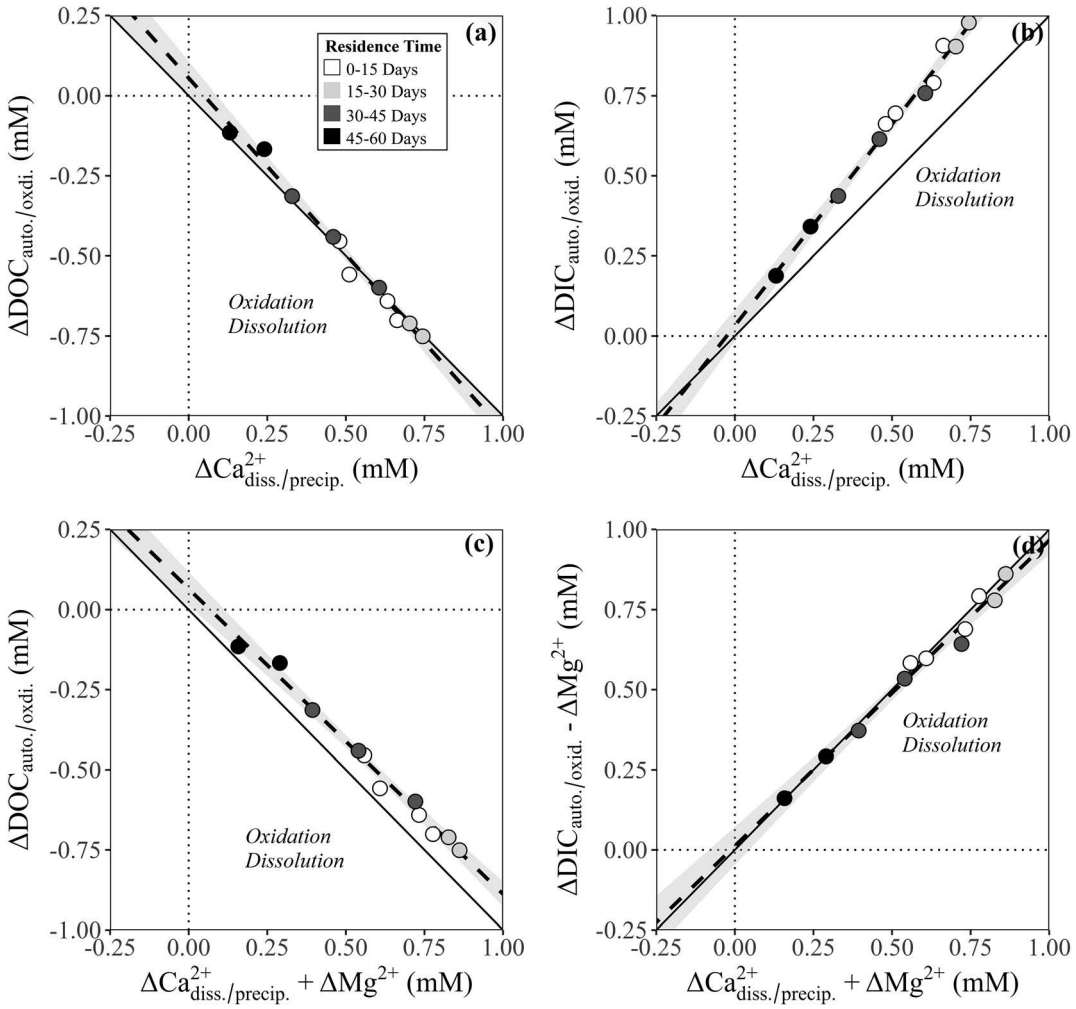

FIGURE 8 Data from a reversal at Madison blue spring. (**a**) ΔDOC values related to oxidation and autotrophy (equation 9) versus ΔCa^{2+} values related to calcite dissolution and precipitation (equation 7), (**b**) ΔDIC values related to oxidation and autotrophy (equation 8) versus ΔCa^{2+} values related to calcite dissolution and precipitation, (**c**) ΔDOC values related to oxidation and autotrophy versus the sum of ΔCa^{2+} and ΔMg^{2+} values (equation 11) and (**d**) ΔDIC values related to oxidation and autotrophy adjusted for ΔMg^{2+} values versus the sum of ΔCa^{2+} and ΔMg^{2+} values. Dotted lines mark Δ[x] values of zero. Data points are shaded according to residence time (key on 'A') and solid lines mark slopes of −1 and 1, respectively. Dashed lines represent linear regressions (Table 1) and the shaded grey regions represent the 0.95 confidence interval.

TABLE 1 Linear regression coefficients and statistical significance.

Site	Relationship	Fig.	Slope	p-value	r^2
Sink-rise system	$\Delta DOC_{auto./oxid.}$ vs $\Delta Ca^{2+}_{diss./precip.}$	7A	−1.79	<0.01	0.72
Sink-rise system	$\Delta DIC_{auto./oxid.}$ vs $\Delta Ca^{2+}_{diss./precip.}$	7B	1.61	<0.01	0.75
Madison Blue Spring	$\Delta DOC_{auto./oxid.}$ vs $\Delta Ca^{2+}_{diss./precip.}$	8A	−1.10	<0.01	0.99
Madison Blue Spring	$\Delta DIC_{auto./oxid.}$ vs $\Delta Ca^{2+}_{diss./precip.}$	8B	1.26	<0.01	0.99
Madison Blue Spring	$\Delta DOC_{auto./oxid.}$ vs $\Delta Ca^{2+}_{diss./precip.} + \Delta Mg^{+}_{diss./precip.}$	8C	−0.95	<0.01	0.99
Madison Blue Spring	$\Delta DIC_{auto./oxid.}$ - $\Delta Mg^{+}_{diss./precip.}$ vs $\Delta Ca^{2+}_{diss./precip.} + \Delta Mg^{+}_{diss./precip.}$	8D	0.95	<0.01	0.98

Blue Spring (Figure 8). $\Delta DOC_{auto/oxid}$ and $\Delta Ca^{2+}_{diss/precip}$ values are inversely correlated at both the sink-rise system and Madison Blue Spring. At both locations, slopes are steeper than −1 and the slope is shallower at Madison Blue Spring than at the sink-rise system (Table 1). Positive $\Delta Ca^{2+}_{diss/precip}$ values are less at the sink-rise system (Figure 7a), where subsurface residence times are < 65 hours (2.7 days), than at Madison Blue Spring, where subsurface residence times were between 3 and 24 days (Figure 8a). $\Delta DIC_{auto/oxid}$ and $\Delta Ca^{2+}_{diss/precip}$ values are positively correlated at both the sink-rise system and Madison Blue Spring with slopes steeper than 1 and the slope is steeper at the sink-rise system than at Madison Blue Spring (Table 1). Significant linear relationships remain at the sink-rise system after correcting for the effects of lag (Supplemental Material).

At the sink-rise system, plots of $\Delta DOC_{auto/oxid}$ versus $\Delta Ca^{2+}_{diss/precip}$ values and $\Delta DIC_{auto/oxid}$ versus $\Delta Ca^{2+}_{diss/precip}$ values indicate a systematic relationship with changing river stage at the time of sample collection (Figure 7). Samples collected on the rising limb of the hydrograph tend to have positive $\Delta Ca^{2+}_{diss/precip}$ and negative $\Delta DOC_{auto/oxid}$ values and plot in the upper left quadrant, while samples collected on the falling limb of a storm event tend to plot in the lower right quadrant (Figure 7a). Samples collected at baseflow tend to cluster near the origin indicating little net change in $\Delta DOC_{auto/oxid}$ or $\Delta Ca^{2+}_{diss/precip}$ values. Similarly, rising limb samples tend to have positive $\Delta Ca^{2+}_{diss/precip}$ and $\Delta DIC_{auto/oxid}$ values and plot in the upper right quadrant, while samples collected on the falling limb tend to have negative $\Delta Ca^{2+}_{diss/precip}$ and $\Delta DIC_{auto/oxid}$ values and plot in the lower left quadrant (Figure 7b). At baseflow, samples tend to have negative $\Delta Ca^{2+}_{diss/precip}$ and $\Delta DIC_{auto/oxid}$ values and overlap with samples collected on the falling limb of the hydrograph. In contrast, samples with 10–25 hour residence times during periods of high flow, cluster at the origin.

At Madison Blue Spring, all samples have positive $\Delta Ca^{2+}_{diss/precip}$, positive $\Delta DIC_{auto/oxid}$ and negative $\Delta DOC_{auto/oxid}$ values (Figure 8). Samples with the longest subsurface residence times plot closest to the origin, and thus have the smallest $\Delta Ca^{2+}_{diss/precip}$, $\Delta DIC_{auto/oxid}$ and $\Delta DOC_{auto/oxid}$ absolute values. Samples of water with an intermediate (15–30 day) subsurface residence time plot furthest from the origin and have the largest $\Delta Ca^{2+}_{diss/precip}$, $\Delta DIC_{auto/oxid}$ and $\Delta DOC_{auto/oxid}$ absolute values.

ΔMg^{2+} values at Madison Blue Spring range from 0.03 to 0.12 mM. After adjusting for potential Mg^{2+} contributions from limestone dissolution (Figure 8c,d), the slope of relationships between $\Delta Ca^{2+}_{diss/precip}$ and $\Delta DOC_{auto/oxid}$ and $\Delta DIC_{auto/oxid}$ values at Madison Blue Spring remain significant but become shallower (Table 1) approaching values of −1 and 1, respectively. The inclusion of ΔMg^{2+} values does not alter relationships with respect to subsurface residence time.

3.4 | C:N ratios and ΔDOC at the sink-rise system and Madison blue spring

At both the sink-rise system and Madison Blue Spring, the ΔC:N ratio shows a positive linear correlation with the ΔDOC value (Figure 9). The sink-rise system shows both positive and negative values for the ΔC:N ratios and ΔDOC values, suggesting periods of net gain and loss of DOC (Figure 8a). An increase in the C:N ratio (positive ΔC:N) is associated with the falling limb of the hydrograph while the largest decrease in the C:N ratio (ΔC:N ratio = ∼ −16) is associated with the rising limb. During baseflow, both decreases and increases in the C:N ratio occur. In contrast, at Madison Blue Spring, all ΔC:N and ΔDOC values are negative. The greatest decrease in the C:N ratio (ΔC:N ratio = ∼ −17) occurs when surface water residence time is between 8 to 20 days and when ΔDOC has a value of about −0.75 mM (Figure 9b). All samples that exhibit smaller decreases in the C:N ratio occur during both shorter and longer subsurface residence times. Both the C:N ratio and DOC concentrations return to baseflow values with increased residence time.

4 | DISCUSSION

In the following discussion, we evaluate diagenetic and microbially mediated reactions caused by surface water-groundwater exchange in carbonate aquifers through modelling changes in Ca^{2+}, DOC and DIC concentrations and C:N molar ratios after adjusting for changes resulting from end-member mixing. Significant linear relationships between these variables support the hypothesis that CO_2 produced from the oxidation of DOC delivered by surface waters enhances limestone dissolution. We explore mechanisms that may influence the slope of these linear relationships, including the influence of CO_2 degassing, Mg^{2+} related to carbonate dissolution, and subsurface residence time, and by inference reaction kinetics. At the sink-rise system, we also consider the relative roles of hydrologic processes and/or autotrophy to cause observed gains in DOC. We also explore how the frequency and duration of groundwater-surface water interactions impact groundwater DOC concentration and C:N ratio in the aquifer around these spring systems.

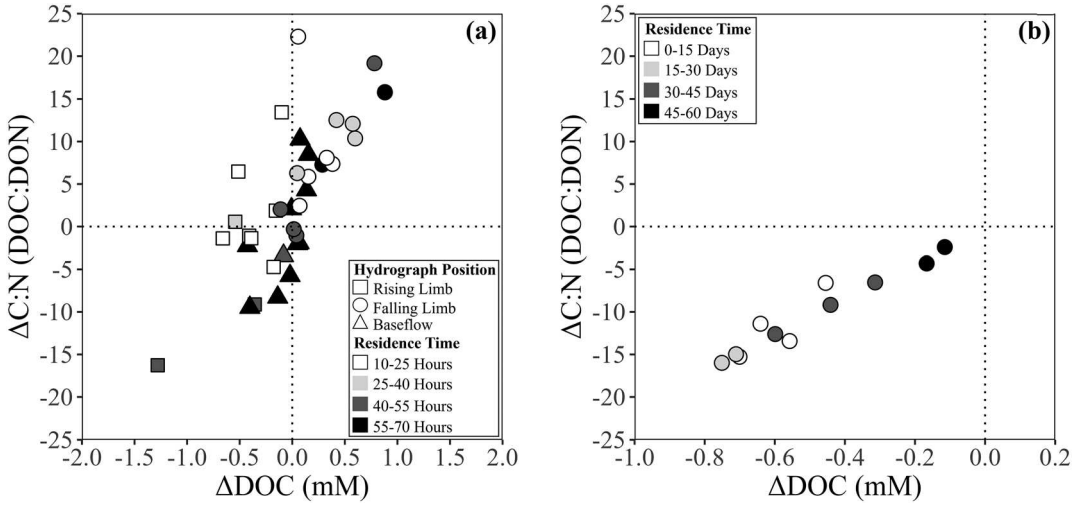

FIGURE 9 Biplot of molar ΔC:N versus ΔDOC at (**a**) the sink-rise system and (**b**) Madison blue spring. Dotted lines mark a Δ value of zero. Point shapes on (A) mark hydrograph position. Points on (a) and (b) are shaded according to residence time.

4.1 | Limestone dissolution driven by OC oxidation

Dissolution of limestone caused by H_2CO_3 production during microbially mediated aerobic oxidation of DOC can be described by the following three reactions:

$$CH_2O + O_2 \rightarrow CO_2 + H_2O \quad (12)$$

$$CO_2 + H_2O \leftrightarrow H_2CO_3 \quad (13)$$

$$CaCO_3 + H_2CO_3 \leftrightarrow Ca^{2+} + 2HCO_3^- \quad (14)$$

Thus, every mole of DOC (as CH_2O) oxidized produces a mole of H_2CO_3 that may dissolve one mole of limestone. If these reactions go to completion, limestone dissolution caused by aerobic DOC oxidation represents the net loss of one mole of DOC (Equation 12) and the net gain of two moles of DIC and one mole of Ca^{2+} (Equation 14). The reverse of reactions 12–14 indicates that autotrophy may result in calcite precipitation. This stoichiometry indicates the relationships of $\Delta DOC_{auto/oxid}$ and $\Delta DIC_{auto/oxid}$ values versus $\Delta Ca^{2+}{}_{diss/precip}$ values should be linear with slopes of −1 and 1, respectively. If these reactions occur during temporary storage in the subsurface, limited light conditions suggest chemolithoautotrophy is the only autotrophic DOC production pathway (e.g., Opsahl & Chanton, 2006).

As microbes oxidize DOC, the hydration of produced CO_2 (Equation 12) is rapid (Ford & Williams, 2007; Roques, 1969) and would support calcite dissolution. Oxidation of DOC should also impact the composition of the residual DOM pool and alter the C:N ratio (i.e. ΔC:N) (Bianchi & Canuel, 2011). Surface water has a C:N ratio higher than spring and well waters (Figure 4b) reflecting a DOM source from C-rich terrestrial plants and woody material composed of lignin and cellulose with C:N ratios > 17 (e.g., Bianchi & Canuel, 2011). In contrast, DOM produced by microbes lacks plant structural components and has greater fractions of proteins and nucleic acids with C:N ratios between 4 and 15 (Bianchi & Canuel, 2011). Our spring and well waters low C:N ratio indicates they contain a larger fraction of microbially produced DOM than the surface waters (e.g., Luzius et al., 2018). Thus, the 2–17 net decrease in the C:N ratio (i.e., negative ΔC:N) associated with net DOC loss at Madison Blue Spring and the sink-rise system (Figure 9) reflects the oxidative loss of terrestrial DOM with elevated C:N ratios in intruding surface waters and a potential simultaneous increase in heterotrophic microbial biomass with low C:N ratios. Hydration of the produced CO_2 drives dissolution and creates the significant inverse linear relationship between $\Delta DOC_{auto/oxid}$ and $\Delta Ca^{2+}{}_{diss/precip}$ values (Figures 7a and 8a). Likewise, DOC oxidation represents a gain of DIC linked to the gain of Ca^{2+} from dissolution (Equations 9 and 14) and creates a significant positive linear relationship between $\Delta DIC_{auto/oxid}$ and $\Delta Ca^{2+}{}_{diss/precip}$ values (Figures 7b and 8b).

Although these observations are from an eogenetic carbonate setting, similar enhanced dissolution from OC oxidation may also occur during point surface water-groundwater interactions in telogenetic carbonates (e.g., Kipper, 2019; Trimboli & Toomey, 2019) but to our knowledge no similar analysis identifying this mechanism in a telogenetic carbonate has been published. Limited primary matrix porosity in telogenetic carbonates would restrict the storage of surface water to existing dissolution and fracture systems and shorten aquifer interaction and subsurface residence time. As discussed below, residence time appears to be important to the extent of reaction progress, and thus short residence time in telogenetic carbonate aquifers would cause reactions to remain farther from completion compared with reactions in eogenetic carbonate aquifers.

4.2 | Possible mechanisms modifying OC oxidation and limestone dissolution stoichiometry

Deviations at the sink-rise system and Madison Blue Spring from the expected slopes of 1 and −1 for $\Delta DOC_{auto/oxid}$ versus $\Delta Ca^{2+}{}_{diss/precip}$ values and $\Delta DIC_{auto/oxid}$ versus $\Delta Ca^{2+}{}_{diss/precip}$ values, respectively (Equations 12–14; Table 1) suggest various processes may modify OC oxidation effects on dissolution reactants and reaction product concentrations. Below we explore these potential processes, including dissolution by acids other than H_2CO_3, the interplay of water residence time and reaction kinetics for CO_2 hydration (Equation 13) and limestone dissolution (Equation 14), slowing reaction kinetics from

armouring of calcite surfaces, effects from degassing of CO_2 and dissolution of Mg-bearing calcite or dolomite (Equation 11).

Dissolution may result from any potential acid source (e.g., equilibrium with atmospheric CO_2, OC oxidation, nitrification, sulphide oxidation, etc.; Covington et al., 2023; Martin, 2017) as surface water recharges the aquifer even following correction for mixing. For example, intruding surface waters are undersaturated with respect to calcite because of equilibration with atmospheric CO_2 (Brown et al., 2014; Gulley et al., 2011; Moore et al., 2010), which will contribute to the total observed dissolution and positive $\Delta Ca^{2+}_{diss/precip}$ values. Thus, the molar relationship should be approximately −1 between $\Delta Ca^{2+}_{diss/precip}$ values and total acid consumed, rather than just the H_2CO_3 consumed. The slope of the relationship between a single acid and $\Delta Ca^{2+}_{diss/precip}$ values is likely to be shallower than −1 depending on the relative concentrations of all acids. Thus, the closer the slope of the relationship between any single acid and $\Delta Ca^{2+}_{diss/precip}$ is to −1 the greater the amount of dissolution from that source.

Instead of slopes shallower than −1, however, observed slopes are steeper than −1 for relationships between $\Delta DOC_{auto/oxid}$ and $\Delta Ca^{2+}_{diss/precip}$ values at both Madison Blue Spring and the sink-rise system (Table 1). These steep slopes indicate greater losses of DOC than corresponding gains of Ca^{2+}, regardless of available acids. The shallower slope at Madison Blue Spring than at the sink-rise system (−1.10 vs − 1.79), despite similar magnitudes of OC oxidation (Figures 7a and 8a), suggests more dissolution occurs for each mole of oxidized DOC. The DOC oxidation must precede dissolution because CO_2 must be produced and hydrated before dissolution can occur. However, DOC oxidation and dissolution can occur simultaneously and thus the greater losses of DOC than corresponding gains of Ca^{2+} indicate the kinetics of dissolution are slower than DOC oxidation and CO_2 hydration. These differences in reaction kinetics coupled with different subsurface residence times allow more DOC oxidation than calcite dissolution. Slower dissolution than oxidation kinetics is supported by larger positive $\Delta Ca^{2+}_{diss/precip}$ values at intermediate residence times (15–30 days) than at short residence time (0–15 days) at Madison Blue Spring (Figure 8a). Intermediate reaction times thus appear to be optimum for maximum DOC oxidation and calcite dissolution. These times are also ~10 times longer than the longest subsurface residence time (2.7 days) for water sampled at River Rise suggesting limited time for calcite dissolution with rapid oxidation (hours) of recharged DOC at both sites. The short reaction times for DOC suggest the consumption of the most labile DOM.

The hydration rate of CO_2 produced from DOC oxidation to H_2CO_3 should not limit limestone dissolution regardless of residence time because outside the diffusion boundary layer equilibrium is reached in bulk liquid within ~5 minutes (Ford & Williams, 2007; Roques, 1969). Instead, rate limitation of dissolution more likely results from the diffusion rate of H^+, Ca^{2+} and HCO_3^- across the boundary layer or the reaction rate of H^+ with available mineral surface sites. Armouring of limestone surfaces would thus decrease limestone dissolution rates at our study sites, depending on the area of reacting minerals (Buhmann & Dreybrodt, 1985a, 1985b). Armouring could result from Fe,Mn-oxide coatings or DOC adsorption, both of which occur at our study sites (Brigmon et al., 1994; Brown et al., 2019; Jin and Zimmerman, 2010; Martin, 1990). The slowed reaction rates from armouring would contribute to greater amounts of dissolution at Madison Blue Spring with longer residence times than the sink-rise system.

Degassing of CO_2 could also contribute to slopes steeper than −1 for $\Delta DOC_{auto/oxid}$ versus $\Delta Ca^{2+}_{diss/precip}$ values by allowing DOC oxidation and CO_2 loss without increasing $\Delta Ca^{2+}_{diss/precip}$ values through dissolution. However, because degassing is not a uniform spatiotemporal process, it is likely to influence individual samples differently and contribute to scatter in the observed linear relationships. Thus, the strong linear correlations at Madison Blue Spring and the presence of only a few outliers at the sink-rise system indicate that CO_2 degassing likely has little impact on the slopes of linear relationships (Figures 7a and 8a). Further, CO_2 concentrations often exceed equilibration with Earth's atmosphere in the vadose zone (Benavente et al., 2010; Gulley et al., 2015; Holden & Fierer, 2005; Mattey et al., 2013; Wong and Banner, 2010; Wood, 1985). These elevated concentrations would also limit CO_2 degassing from injected surface water (e.g., Gulley, Martin, Moore, & Murphy, 2013).

Deviation from expected slope values may result from the dissolution of Mg-rich carbonate or dolomite rather than pure calcite dissolution. Including ΔMg^{2+} in the molar relationships (Equation 11) at Madison Blue Spring results in the expected slope values shallower than −1 for $\Delta DOC_{auto/oxid}$ versus $\Delta Ca^{2+}_{diss/precip}$ values (i.e. $\Delta Ca^{2+}_{diss/precip} + \Delta Mg^{2+}$) values and near 1 for $\Delta DIC_{auto/oxid}$ (i.e., $\Delta DIC_{auto/oxid}$ - ΔMg^{2+}) (Figure 8c,d; Table 1). However, the slope of −0.95 for $\Delta DOC_{auto/oxid}$ versus $\Delta Ca^{2+}_{diss/precip} + \Delta Mg^{2+}$ values, in other words, the ratio of a single acid source to total dissolution, suggests 95% of dissolution is caused by OC oxidation during the reversal at Madison Blue Spring. Such a high contribution to total dissolution is unrealistic considering calcite saturation indices show undersaturation between −2.7 and −4.5 for intruding surface waters during reversal (Brown et al., 2014; Gulley et al., 2011), which is likely to account for more than 5% of dissolution. This unrealistic contribution supports the previous conclusion of a more rapid rate of OC oxidation than of dissolution. Dissolution of Mg^{2+}-bearing minerals also likely occurs at the sink-rise system but our mixing model, which includes Mg^{2+} as a component, precludes an analysis similar to the one at Madison Blue Spring. However, contributions from Mg-bearing carbonates are probably sufficiently small to prevent correcting the slopes to their expected values.

4.3 | Potential autotrophy or storage at the sink-rise system

The $\Delta DOC_{auto/oxid}$ and $\Delta DIC_{auto/oxid}$ versus $\Delta Ca^{2+}_{diss/precip}$ relationships at the sink-rise system suggest autotrophy increases DOC concentrations (Figure 7). Autotrophy would simultaneously sequester CO_2 (reverse Equation 11), reduce acidity and cause calcite precipitation depending on its original saturation state. These changes would result in the linear correlations observed between Ca^{2+} concentrations and oxidized and reduced forms of carbon. Any autotrophy would be expected to decrease C:N ratios of the DOC by increasing the concentrations of N-rich proteins and nucleic acids (e.g., Bianchi & Canuel, 2011; Bronk et al., 1998).

Against expectations, however, samples showing positive ΔDOC and negative $\Delta DIC_{auto/oxid}$ values indicating autotrophy have corresponding increases in C:N ratios (Figures 7b and 9a). One

explanation for this result is that most samples with elevated ΔDOC values were collected on the falling limb of the hydrograph when flood water stored in the matrix porosity flows back to the conduit system. Initially, this surface-derived water would contain elevated DOC concentrations that alter the baseflow matrix water compositions and thus would not be considered in the mixing calculation. During storage in the aquifer matrix, heterotrophy would preferentially remove the most labile terrestrial DOM, typically smaller molecules with lower C:N, leaving the residual DOM more recalcitrant with elevated C:N ratios. Any decrease in C:N ratios from autotrophy would be overwhelmed by a large residual pool of terrestrial DOM with elevated C:N ratios.

The observed increase in the C:N ratio may also reflect preferential adsorption and subsequent desorption of large high molecular weight humic-like DOM with elevated C:N ratios from aquifer material. As surface water is injected into the aquifer matrix on the rising limb of the hydrograph, high C:N ratio DOM adsorbs to the rock surfaces. During the flood recession, as temporarily stored water returns to the conduit system and DOM concentrations decrease, the high C:N molecules would desorb. However, this process probably provides a minimal effect, considering the magnitude of DOM sorption is small for UFA rock (Jin & Zimmerman, 2010).

4.4 | Long term impact of groundwater-surface water interactions on springs

Groundwater from wells at the sink-rise system, which is ~0.3 to 1 km from the mapped conduits, has elevated median DOC concentrations and C:N ratios that suggest a terrestrial OC origin (Figure 4). These concentrations indicate the presence of local pools of elevated terrestrial DOM in the groundwater (Figure 2). The source of this terrestrial DOM is likely the continuous input of surface water at River Sink, which exchanges with the surrounding aquifer matrix during flow through the conduits connected to River Rise (Martin & Dean, 2001). Elevated terrestrial DOM in groundwater far from the conduits implies some fraction of the water recharging at River Sink and into the aquifer, matrix does not return to the conduits as head gradients between the conduit and matrix porosity reverse and instead mixes into local or regional groundwater flow systems. The loss of recharged water would not alter individual solute concentrations and would thus change all Δ[x] values equally, with no impact on mixing model estimates. The elevated DOC of the aquifer matrix likely promotes greater localized dissolution as DOC is oxidized (Gulley et al., 2014, 2016, 2020).

Conversely, the less frequent intrusion of surface water at reversing springs appears to have minimal long-term impact on the DOC concentration or the C:N ratio of local groundwater (Figure 4). Baseflow DOC concentrations and C:N ratios at reversing springs are similar to regional Floridan aquifer groundwater (e.g., McMahon et al., 2017) and the Ichetucknee Spring system, which is dominated by diffuse recharge without spring reversals (Martin et al., 2016). This observation also implies that little of the surface water injected during spring reversals escapes to the regional groundwater flow system. Alternatively, the minor amount of DOC from injected surface water that leaves local systems may be oxidized prior to discharge at springs that do not experience reversals.

As indicated by this work, as well as others (Grünheid et al., 2005; Fonseca et al., 2014; Liu et al., 2021), portions of recharged terrestrial DOM can be oxidized in hours to weeks. This oxidation limits concentrations of DOC in regions of aquifers far from locations of point recharge, for example where springs reverse flow or proximal to sinking streams. This oxidation should decrease C:N ratios, but C:N ratios of some baseflow reversing springs and Ichetucknee spring and well water are anomalously low (<4). These low values may be an artefact of concentrations near detection limit concentrations of DOC, TDN and inorganic nitrogen species. Nonetheless, the C:N ratio of DOM with long residence times in diffusely recharged groundwater is lower than in regions that have frequent spring reversals and sink-rise system waters.

Differences in DOC concentrations between regional groundwater systems with diffuse recharge through the land surface and localized areas influenced by point surface water recharge emphasize the importance of various controls on aquifer carbon cycling in karst regions. Point recharge events represent a major energy flux to oligotrophic aquifer environments and result in the transformation of terrestrial OC to DIC and the release of inorganic carbon sequestered in solid phases via enhanced carbonate dissolution. However, these changes depend on the amount of time available for reactions to reach completion. A portion of the oxidized carbon will return as CO_2 to the atmosphere. Over human time scales, these surface water-groundwater interactions likely represent a substantial portion of the carbon cycling that occurs in carbonate aquifers and associated surface waters. This carbon cycling in carbonate karst landscapes should be considered in estimates of the global carbon cycle (e.g., Liu et al., 2011; Martin, 2017).

5 | CONCLUSIONS

Significant ($p < 0.01$) linear relationships occur between changes in DOC, Ca^{2+} and DIC concentrations of water samples collected during groundwater-surface water interactions at a reversing spring and a stream sink-rise system in north-central Florida. These relationships reflect the oxidation of OC supplied by intruding surface waters coupled with dissolution by H_2CO_3 during temporary storage in the aquifer. Losses of DOC are inversely and linearly correlated with gains of Ca^{2+} at both the reversing spring and the stream sink-rise system. The slope of the relationship is steeper than the expected value of -1 at both systems but closer to -1 at the reversing spring, which has longer subsurface residence times than at the sink-rise system. These results suggest a kinetic control as faster OC oxidation and H_2CO_3 production than carbonate dissolution fractionates the reaction products. Consequently, longer subsurface residence times at the reversing spring (weeks to months) than the sink-rise system (hours to days) allow OC oxidation to contribute a greater amount of dissolution. Continuous recharge at the sink-rise system increases the regional groundwater DOC concentration while stochastic intrusions at the reversing spring do not have long-term impacts on the local groundwater DOC concentration and composition. Our findings support the role of OC oxidation in dissolution of carbonate aquifers but depend on the mechanism, timing and magnitude of surface water recharge. Importantly, mechanisms of point recharge focus on dissolution and thus represent an important source of further speleogenesis and a key location of carbon cycling.

ACKNOWLEDGEMENTS

We acknowledge financial support for this work from the Cave Research Foundation and the University of Florida. Additional support was provided by the National Science Foundation under Grant EAR-1905259. We appreciate the permission to sample springs from the Florida Department of Environmental Protection (permit number 08122212) and the assistance of personnel at Florida State Parks and the Suwannee River Water Management District. Thanks to Alex Janelle and Adrian Barry-Sosa for assistance with field work and to Jason Curtis, George Kamenov and Ray Thomas for assistance with sample analysis.

ORCID

Andrew Oberhelman https://orcid.org/0000-0002-4231-7562

REFERENCES

Bailly-Comte, V., Martin, J.B., Jourde, H., Screaton, E., Pistre, S. & Langston, A.L. (2010) Water exchange and pressure transfer between conduits and matrix and their influence on hydrodynamics of two karst aquifers with sinking streams. *Journal of Hydrology*, 386(1–4), 55–66. Available from: https://doi.org/10.1016/j.jhydrol.2010.03.005

Bailly-Comte, V., Martin, J.B. & Screaton, E. (2011) Time variant cross correlation to assess residence time of water and implication for hydraulics of a sink-rise karst system. *Water Resources Research*, 47(5), 1–16. Available from: https://doi.org/10.1029/2010wr009613

Baldini, J.U., Baldini, L.M., McDermott, F. & Clipson, N. (2006) Carbon dioxide sources, sinks, and spatial variability in shallow temperate zone caves: evidence from Ballynamintra cave, Ireland. *Journal of Cave and Karst Studies*, 68(1), 4–11.

Benavente, J., Vadillo, I., Carrasco, F., Soler, A., Liñán, C. & Moral, F. (2010) Air carbon dioxide contents in the vadose zone of a Mediterranean karst. *Vadose Zone Journal*, 9(1), 126. Available from: https://doi.org/10.2136/vzj2009.0027

Bianchi, T.S. & Canuel, E.A. (2011) *Chemical biomarkers in aquatic ecosystems*. New Jersey: Princeton University Press.

Bögli, A. (1964) Mischungskorrosion - Ein Beitrag zum Verkarstungsproblem. *Erdkunde*, 18(2), 83–92. Available from: https://doi.org/10.3112/erdkunde.1964.02.02

Brigmon, R.L., Martin, H.W., Morris, T., Bitton, G. & Zam, S.G. (1994) Biogeochemical ecology of Thiothrixspp. In underwater limestone caves. *Geomicrobiology Journal*, 12(3), 141–159. Available from: https://doi.org/10.1080/01490459409377982

Bronk, D.A., Glibert, P.M., Malone, T.C., Banahan, S. & Sahlsten, E. (1998) Inorganic and organic nitrogen cycling in Chesapeake Bay: autotrophic versus heterotrophic processes and relationships to carbon flux. *Aquatic Microbial Ecology*, 15, 177–189. Available from: https://doi.org/10.3354/ame015177

Brown, A.L., Martin, J.B., Kamenov, G.D., Ezell, J., Screaton, E., Gulley, J., et al. (2019) Trace metal cycling in karst aquifers subject to periodic river water intrusion. *Chemical Geology*, 527, 118773. Available from: https://doi.org/10.1016/j.chemgeo.2018.05.020

Brown, A.L., Martin, J.B., Screaton, E., Ezell, J., Spellman, P. & Gulley, J. (2014) Bank storage in karst aquifers: the impact of temporary intrusion of river water on carbonate dissolution and trace metal mobility. *Chemical Geology*, 385, 56–69. Available from: https://doi.org/10.1016/j.chemgeo.2014.06.015

Budd, D.A. & Vacher, H.L. (2004) Matrix permeability of the confined Floridan aquifer, Florida, USA. *Hydrogeology Journal*, 12(5), 531–549. Available from: https://doi.org/10.1007/s10040-004-0341-5

Buhmann, D. & Dreybrodt, W. (1985a) The kinetics of calcite dissolution and precipitation in geologically relevant situations of karst areas: 1. Open system. *Chemical Geology*, 48(1–4), 189–211. Available from: https://doi.org/10.1016/0009-2541(85)90046-4

Buhmann, D. & Dreybrodt, W. (1985b). The kinetics of calcite dissolution and precipitation in geologically relevant situations of karst areas: 2. Closed system. *Chemical Geology*, 53(1–2),109–124. Available from: https://doi.org/10.1016/0009-2541(85)90024-5

Choquette, P. & Pray, L. (1970) Geologic nomenclature and classification of porosity in sedimentary carbonates. *AAPG Bulletin*, 54, 207–250. Available from: https://doi.org/10.1306/5d25c98b-16c1-11d7-8645000102c1865d

Cooper, K., Whitaker, F.F., Anesio, A.M., Naish, M., Reynolds, D.M. & Evans, E.L. (2016) Dissolved organic carbon transformations and microbial community response to variations in recharge waters in a shallow carbonate aquifer. *Biogeochemistry*, 129(1–2), 215–234. Available from: https://doi.org/10.1007/s10533-016-0226-4

Covington, M.D., Martin, J.B., Toran, L., Macalady, J.L., Sekhon, N., Sullivan, P.L., et al. (2023) Carbonates in the critical zone. *Earth's Future*, 11(1), 1–31. Available from: https://doi.org/10.1029/2022ef002765

Dreybrodt, W. & Romanov, D. (2007) Time scales in the evolution of solution porosity in porous coastal carbonate aquifers by mixing corrosion in the saltwater-freshwater transition zone. *Acta Carsologica*, 36(1), 25–34. Available from: https://doi.org/10.3986/ac.v36i1.205

Fonseca, A.L.D.S., Bianchini, I., Pimenta, C.M.M., Mangiavacchi, N. & Soares, C.B.P. (2014) Kinetics of aerobic decomposition in the leaching phase of allochthonous plant detritus. *Acta Limnologica Brasiliensia*, 26(1), 89–97. Available from: https://doi.org/10.1590/s2179-975x2014000100010

Ford, D. & Williams, P.W. (2007) *Karst hydrogeology and geomorphology*. Chichester: John Wiley & Sons.

Gabrovšek, F. & Dreybrodt, W. (2010) Karstification in unconfined limestone aquifers by mixing of phreatic water with surface water from a local input: a model. *Journal of Hydrology*, 386(1–4), 130–141. Available from: https://doi.org/10.1016/j.jhydrol.2010.03.015

Grünheid, S., Amy, G.L. & Jekel, M. (2005) Removal of bulk dissolved organic carbon (DOC) and trace organic compounds by bank filtration and artificial recharge. *Water Research*, 39(14), 3219–3228. Available from: https://doi.org/10.1016/j.watres.2005.05.030

Gulley, J., Breecker, D.O., Covington, M.D., Cooperdock, S., Banner, J.L., Moore, P., et al. (2020) Tidal pumping and biogeochemical processes: dissolution within the tidal capillary fringe of eogenetic coastal carbonates. *Earth Surface Processes and Landforms*, 45(11), 2675–2688. Available from: https://doi.org/10.1002/esp.4922

Gulley, J., Martin, J.B. & Brown, A.L. (2016) Organic carbon inputs, common ions and degassing: rethinking mixing dissolution in coastal eogenetic carbonate aquifers. *Earth Surface Processes and Landforms*, 41(14), 2098–2110. Available from: https://doi.org/10.1002/esp.3975

Gulley, J., Martin, J.B. & Moore, P. (2014) Vadose CO_2 gas drives dissolution at water tables in eogenetic karst aquifers more than mixing dissolution. *Earth Surface Processes and Landforms*, 39(13), 1833–1846. Available from: https://doi.org/10.1002/esp.3571

Gulley, J., Martin, J., Moore, P., Brown, A.L., Spellman, P. & Ezell, J. (2015) Heterogeneous distributions of CO_2 may be more important for dissolution and karstification in coastal eogenetic limestone than mixing dissolution. *Earth Surface Processes and Landforms*, 40(8), 1057–1071. Available from: https://doi.org/10.1002/esp.3705

Gulley, J., Martin, J.B., Moore, P. & Murphy, J. (2013) Formation of phreatic caves in an eogenetic karst aquifer by CO_2 enrichment at lower water tables and subsequent flooding by sea level rise. *Earth Surface Processes and Landforms*, 38(11), 1210–1224. Available from: https://doi.org/10.1002/esp.3358

Gulley, J., Martin, J.B., Screaton, E. & Moore, P. (2011) River reversals into karst springs: A model for cave enlargement in eogenetic karst aquifers. *Geological Society of America Bulletin*, 123(3–4), 457–467. Available from: https://doi.org/10.1130/b30254.1

Gulley, J., Martin, J.B., Spellman, P., Moore, P. & Screaton, E. (2013) Dissolution in a variably confined carbonate platform: effects of allogenic runoff, hydraulic damming of groundwater inputs, and surface-groundwater exchange at the basin scale. *Earth Surface Processes and Landforms*, 38(14), 1700–1713. Available from: https://doi.org/10.1002/esp.3411

Holden, P.A. & Fierer, N. (2005) Microbial processes in the vadose zone. *Vadose Zone Journal*, 4(1), 1–21. Available from: https://doi.org/10.2136/vzj2005.0001

Jin, J. & Zimmerman, A.R. (2010) Abiotic interactions of natural dissolved organic matter and carbonate aquifer rock. *Applied Geochemistry*, 25(3), 472–484. Available from: https://doi.org/10.1016/j.apgeochem.2009.12.012

Katz, B.G., Böhlke, J.K. & Hornsby, H.D. (2001) Timescales for nitrate contamination of spring waters, northern Florida, USA. *Chemical Geology*, 179(1–4), 167–186. Available from: https://doi.org/10.1016/S0009-2541(01)00321-7

Khadka, M.B., Martin, J.B. & Jin, J. (2014) Transport of dissolved carbon and CO_2 degassing from a river system in a mixed silicate and carbonate catchment. *Journal of Hydrology*, 513, 391–402. Available from: https://doi.org/10.1016/j.jhydrol.2014.03.070

Kipper, C. (2019) *Influence of spring flow reversals on cave dissolution in a influence of spring flow reversals on cave dissolution in a Telogenetic karst aquifer, mammoth cave, KY Telogenetic karst aquifer, mammoth cave, KY [MS thesis]*. Bowling Green: Western Kentucky University.

Liu, J., Liang, J., Bravo, A.G., Wei, S., Yang, C., Wang, D. & Jiang, T. (2021) Anaerobic and aerobic biodegradation of soil-extracted dissolved organic matter from the water-level-fluctuation zone of the Three Gorges Reservoir region, China. *Science of The Total Environment*, 764, 1–11. Available from: https://doi.org/10.1016/j.scitotenv.2020.142857

Liu, Z., Dreybrodt, W. & Liu, H. (2011) Atmospheric CO2 sink: silicate weathering or carbonate weathering? *Applied Geochemistry*, 26, S292–S294. Available from: https://doi.org/10.1016/j.apgeochem.2011.03.085

Luzius, C., Guillemette, F., Podgorski, D.C., Kellerman, A.M. & Spencer, R.G.M. (2018) Drivers of dissolved organic matter in the vent and major conduits of the world's largest freshwater spring. *Journal of Geophysical Research – Biogeosciences*, 123(9), 2775–2790. Available from: https://doi.org/10.1029/2017jg004327

Martin, H.W. (1990) Phreatite: a speleothem formed in phreatic limestone conduits. *Underwater Speleology*, 17(6), 6–10.

Martin, J.B. (2017) Carbonate minerals in the global carbon cycle. *Chemical Geology*, 449, 58–72. Available from: https://doi.org/10.1016/j.chemgeo.2016.11.029

Martin, J.B. & Dean, R.W. (1999) Temperature as a natural tracer of short residence times for groundwater in karst aquifers. In: Palmer, A.N., Palmer, M.V. & Sasowsky, I.D. (Eds.) *Special publication 5: karst modeling*. Lewisburg: Karst Waters Institute, pp. 236–242.

Martin, J.B. & Dean, R.W. (2001) Exchange of water between conduits and matrix in the Floridan aquifer. *Chemical Geology*, 179(1–4), 145–165. Available from: https://doi.org/10.1016/s0009-2541(01)00320-5

Martin, J.B., Kurz, M.J. & Khadka, M.B. (2016) Climate control of decadal-scale increases in apparent ages of eogenetic karst spring water. *Journal of Hydrology*, 540, 988–1001. Available from: https://doi.org/10.1016/j.jhydrol.2016.07.010

Martin, J.M., Screation, E.J. & Martin, J.B. (2006) Monitoring well responses to karst conduit head fluctuations: Implications for fluid exchange and matrix transmissivity in the Floridan aquifer. In: Harmon, R.S. & Wicks, C.M. (Eds.) *Perspectives on karst geomorphology, hydrology, and geochemistry - a tribute volume to Derek C. Ford and William B. White*. Boulder: Geological Society of America, pp. 209–217. Available from: https://doi.org/10.1130/2006.2404(17)

Mattey, D., Fisher, R.E., Atkinson, T.C., Latin, J., Durrell, R., Ainsworth, M., et al. (2013) Methane in underground air in Gibraltar karst. *Earth and Planetary Science Letters*, 374, 71–80. Available from: https://doi.org/10.1016/j.epsl.2013.05.011

McMahon, P.B., Belitz, K., Barlow, J.R.B. & Jurgens, B.C. (2017) Methane in aquifers used for public supply in the United States. *Applied Geochemistry*, 84, 337–347. Available from: https://doi.org/10.1016/j.apgeochem.2017.07.014

Meinzer, O.E. (1927) *Large springs in the United States, water supply paper 557*. Washington, DC: Unites States Geological Survey.

Moore, P.J., Martin, J.B. & Screaton, E.J. (2009) Geochemical and statistical evidence of recharge, mixing, and controls on spring discharge in an eogenetic karst aquifer. *Journal of Hydrology*, 376(3–4), 443–455. Available from: https://doi.org/10.1016/j.jhydrol.2009.07.052

Moore, P., Martin, J.B., Screaton, E.J. & Neuhoff, P.S. (2010) Conduit enlargement in an eogenetic karst aquifer. *Journal of Hydrology*, 393(3–4), 143–155. Available from: https://doi.org/10.1016/j.jhydrol.2010.08.008

Mylroie, J.E. & Carew, J.L. (1990) The flank margin model for dissolution cave development in carbonate platforms. *Earth Surface Processes and Landforms*, 15(5), 413–424. Available from: https://doi.org/10.1002/esp.3290150505

Opsahl, S.P. & Chanton, J.P. (2006) Isotopic evidence for methane-based chemosynthesis in the Upper Floridan aquifer food web. *Oecologia*, 150(1), 89–96. Available from: https://doi.org/10.1007/s00442-006-0492-2

Palmer, A.N. (1991) Origin and morphology of limestone caves. *Geological Society of America Bulletin*, 103(1), 1–21. Available from: https://doi.org/10.1130/0016-7606(1991)103<0001:oamolc>2.3.co;2.

Ritorto, M., Screaton, E., Martin, J.B. & Moore, P. (2009) Relative importance and chemical effects of diffuse and focused recharge in an eogenetic karst aquifer: an example from the unconfined upper Floridan aquifer, USA. *Hydrogeology Journal*, 17(7), 1,687–1,698. Available from: https://doi.org/10.1007/s10040-009-0460-0

Roques, H. (1969) Problemes de transfert de masse pose par l'evolution des eaux souterraines. *Annales De Spéléologie*, 24(3), 455–494.

Sanford, W.E. & Konikow, L.F. (1989) Porosity development in coastal carbonate aquifers. *Geology*, 17(3), 249–252. Available from: https://doi.org/10.1130/0091-7613(1989)017

Schmidt, W., Hoenstine, R.W., Knapp, M.S., Lane, E., Ogden, G.M. & Scott, T.M. (1979) *The limestone, dolomite and coquina resources of Florida. Report of investigation 88*. Tallahassee, Florida: Bureau of Geology, Division of Resource Management, Florida Department of Natural Resources.

Scott, T.M. (1988) *The lithostratigraphy of the hawthorn group (Miocene) of Florida (FGS: bulletin 59)*. Tallahassee: Florida Geological Survey Available from: https://ufdc.ufl.edu/UF00000226/00001

Screaton, E., Martin, J.B., Ginn, B.K. & Smith, L.C. (2004) Conduit properties and karstification in the unconfined Floridan aquifer. *Ground Water*, 42(3), 338–346. Available from: https://doi.org/10.1111/j.1745-6584.2004.tb02682.x

Trimboli, S.R. & Toomey, R. (2019) Temperature and reverse-flow patterns of the river Styx, mammoth cave, Kentucky. *Journal of Cave and Karst Studies*, 81(3), 153–161. Available from: https://doi.org/10.4311/2017es0106

Vacher, H.L. & Mylroie, J.E. (2002) Eogenetic karst from the perspective of an equivalent porous medium. *Carbonates and Evaporites*, 17(2), 182–196. Available from: https://doi.org/10.1007/bf03176484

Whitaker, F.F. & Smart, P.L. (2007) Geochemistry of meteoric diagenesis in carbonate islands of the northern Bahamas: 1. Evidence from field studies. *Hydrological Processes*, 21(7), 949–966. Available from: https://doi.org/10.1002/hyp.6532

Williams, L.J. & Kuniansky, E.L. (2015) *Revised hydrogeologic framework of the Floridan aquifer system in Florida and parts of Georgia, Alabama, and South Carolina*. Washington, DC: U.S. Geological Survey Professional Paper.

Wong, C.I. & Banner, J.L. (2010) Response of cave air CO_2 and drip water to brush clearing in Central Texas: implications for recharge and soil CO_2 dynamics. *Journal of Geophysical Research*, 115(G4), 1–13. Available from: https://doi.org/10.1029/2010jg001301

Wood, W.W. (1985) Origin of caves and other solution openings in the unsaturated (vadose) zone of carbonate rocks: a model for CO_2 generation. *Geology*, 13(11), 822. Available from: https://doi.org/10.1130/0091-7613(1985)13

SUPPORTING INFORMATION

Additional supporting information can be found online in the Supporting Information section at the end of this article.

How to cite this article: Oberhelman, A., Martin, J.B. & Flint, M.K. (2024) Groundwater-surface water interaction, dissolved organic carbon oxidation and dissolution in carbonate aquifers. *Earth Surface Processes and Landforms*, 49(8), 2311–2325. Available from: https://doi.org/10.1002/esp.5830